Anal. Chem. **2009,** *81,* 7243–7247

Plasmon-Induced Enhancement in Analytical Performance Based on Gold Nanoparticles Deposited on TiO_2 Film

Anwei Zhu, Yongping Luo, and Yang Tian*

Department of Chemistry, Tongji University, Siping Road 1239, Shanghai 200092, People's Republic of China

This paper demonstrates a novel approach for developing the analytical performance of electrochemical biosensors in which hydrogen peroxide (H_2O_2) is selected as a model target, based on surface plasmon resonance of gold nanoparticles (Au NPs) deposited onto a TiO_2 nanoneedle film. Direct electron transfer of cytochrome c (cyt. c) is realized at Au NPs deposited onto a TiO_2 nanoneedle film (Au/TiO_2 film), and both anodic and cathodic currents of the redox reaction at the Au/TiO_2 film upon visible-light irradiation are amplified. Meanwhile, in the presence of oxidized or reduced states of cyt. c, cathodic or anodic photocurrents are generated respectively by the Au/TiO_2 film, suggesting that the amplified anodic and cathodic currents are ascribed to the visible-light excitation. The photocurrent action spectrum obtained at the Au/TiO_2 film in the presence of cyt. c is in a good agreement with the surface plasmon absorption spectrum of Au NPs deposited onto the TiO_2 film, and maximum photocurrent is also consistent with the plasmon absorption peak of Au NPs themselves. It indicates that the enhanced photocurrents generated by visible-light irradiation are attributed to the surface plasmon resonance of Au NPs. On the other hand, experimental results reveal that cyt. c is stably immobilized onto the Au/TiO_2 film and maintains inherent enzymatic activity toward H_2O_2 even under continuous visible-light illumination. The amplified redox currents of cyt. c produced by surface plasmon resonance of Au NPs, combined with the stability and enzymatic activity of cyt. c confined on the Au/TiO_2 film even after continuous visible-light illumination, subsequently provide the enhanced analytical performance in determination of H_2O_2. The sensitivity of the present biosensor for H_2O_2 is 4-fold larger than that obtained without visible-light irradiation, the detection limit is achieved to be 4.5×10^{-8} M and the dynamic detection linear range extends from 1×10^{-7} M to 1.2×10^{-2} M.

In the past few years, an intensive research effort has been devoted to the field of electrochemical biosensors capable of providing better analytical performance, in terms of sensitivity, selectivity, stability, reproducibility, and so on.[1] The gold nanoparticles (Au NPs) with unique chemical and physical properties are extremely suitable for designing new sensing devices.[2] Indeed, the biocompatibility and large surface area of Au NPs provide a favorable microenvironment for adsorption of biomolecules without denaturation.[3] Furthermore, Au NPs have been employed either to act as an electron transfer bridge for direct electrical contacting of redox proteins with electrode supports or to play the crucial role in both immunosensors and DNA sensors.[4,5] All these features of Au NPs constitute useful strategies for the preparation of biosensors with developed analytical performance.

Another important characteristic of Au NPs is going along with their localized surface plasmon resonance (LSPR), which is due to the collective oscillations of conductive electrons induced by the electric field of visible light. The changes of plasmon resonance wavelength upon the refractive index of Au NPs have provided a convenient method for label-free detection of biomolecular.[6] Moreover, the resonant interaction between the surface charge oscillation and the electromagnetic field of visible light has been reported to result in an enhancement of the optical signals from molecules.[7] Typical examples include metal fluorescence[8] and surface-enhanced Raman scattering[9] with enhancement factors large enough either to allow single molecular detection[10] or to enhance second-harmonic generation of adsorbed molecules.[11] A further plasmon-induced photoelectrochemistry has been investigated at Au NPs deposited onto TiO_2 film and

* To whom correspondence should be addressed. Tel.: +86-21-65987075. Fax: +86-21-65982287. E-mail: yangtian@mail.tongji.edu.cn.

(1) (a) Murray, R. W. *Chem. Rev.* **2008**, *108*, 2688–2720. (b) Gill, R.; Zayats, M.; Willner, I. *Angew. Chem., Int. Ed.* **2008**, *47*, 7602–7625. (c) Xue, X.; Wang, J.; Li, Q.; Yan, Y.; Liu, J.; Cai, W. *Anal. Chem.* **2008**, *80*, 166–171.
(2) (a) Daniel, M. C.; Astruc, D. *Chem. Rev.* **2004**, *104*, 293–346. (b) Zamborini, F. P.; Leopold, M. C.; Hicks, J. F.; Kulesza, P. J.; Malik, M. A.; Murray, R. W. *J. Am. Chem. Soc.* **2002**, *124*, 8958–8964.
(3) Jia, J.; Wang, B.; Wu, A.; Cheng, G.; Li, Z.; Dong, S. *Anal. Chem.* **2002**, *74*, 2217–2223.
(4) Xiao, Y.; Patolsky, F.; Katz, E.; Hainfeld, J. F.; Willner, I. *Science* **2003**, *299*, 1877–1881.
(5) Dequaire, M.; Degrand, C.; Limoges, B. *Anal. Chem.* **2000**, *72*, 5521–5528.
(6) (a) Jain, P. K.; Huang, X.; El-Sayed, I. H.; El-Sayed, M. A. *Plasmonics* **2007**, *2*, 107–118. (b) Hong, S.; Choi, I.; Lee, S.; Yang, Y. I.; Kang, T.; Yi, J. *Anal. Chem.* **2009**, *81*, 1378–1382.
(7) Chen, C. K.; Heinz, T. F.; Ricard, D.; Shen, Y. R. *Phys. Rev. B: Condens. Matter* **1983**, *27*, 1965–1979.
(8) Aslan, K.; Lakowicz, R. J.; Szmacinki, H.; Geddes, D. C. *J. Fluoresc.* **2004**, *14*, 677–679.
(9) (a) Moskovits, M. *Rev. Mod. Phys.* **1985**, *57*, 783–826. (b) Schatz, G. C. *Acc. Chem. Res.* **1984**, *17*, 370–376.
(10) Nie, S. M.; Emory, S. R. *Science* **1997**, *275*, 1102–1106.
(11) Quail, C.; Rako, C.; Simon, J.; Deck, R. *Phys. Rev. Lett.* **1983**, *50*, 1987–1989.

10.1021/ac900894p CCC: $40.75
Published on Web 08/05/2009

developed for applications in photovoltaic cells,[12] photocatalysts[12b,13] and surface patterning.[14] The mechanism of electron transfer from Au NPs to nanocrystalline TiO_2 has also been proven by femtosecond transient absorption spectroscopy with infrared (IR) probe[15] and steady-state ultraviolet-visible-light (UV−vis) spectroscopy.[16]

However, to the best of our knowledge, the conjugation of plasmon-induced photocurrents with enhanced analytical performance in electrochemical biosensors has never been reported. In the present work, a novel route has been achieved for developing analytical performance of electrochemical biosensors based on surface plasmon resonance of gold nanoparticles deposited onto a film of TiO_2 nanoneedles. Direct electron transfer of cyt. c has been realized at the Au/TiO_2 film, and both anodic and cathodic currents of the redox reaction have been amplified upon visible-light irradiation. In addition to the stability and enzymatic activity of cyt. c confined on the Au/TiO_2 film, the amplified redox currents of cyt. c produced by surface plasmon resonance of Au NPs have provided the enhanced analytical performance in determination of H_2O_2. The present approach should be an alternative contribution to electrochemical biosensors, because the sensitivity and other analytical characteristics of electrochemical responses toward analytes have been improved by not only electrode potential but also surface plasmon resonance. Moreover, Au NPs have demonstrated an additional advantage in this case, because they undergo charge separation upon irradiation with visible light, which imposes less damage on the biomolecules adsorbed on the electrode than UV illumination.

EXPERIMENTAL SECTION

Reagents and Materials. Horse heart cytochrome c (cyt. c, MW 12 384) and hydrogen tetrachloroaurate(III) tetrahydrate were purchased from Sigma−Aldrich. The reduced form of cyt. c on the modified electrode was generated by applying potentials of −0.18 V vs Ag/AgCl on the surface-bound cyt. c for 200 s.[17] Gold nanoparticles suspended in solution was prepared by the method previously reported.[18] TiO_2 nanoneedles (FT-2000) were obtained from Ishihara Sangyo Kaisha. Indium tin oxide (ITO)-coated glass plates with a square resistance of ~10 Ω/cm^2 were purchased from Shenzhen Nanbo Display Technology Co., Ltd. All other reagents were of analytical grade, and doubly distilled water was used throughout.

Preparation and Modification. A highly conductive ITO electrode that had been coated with a TiO_2 film was prepared from a sol of TiO_2 nanoneedles by spin-coating, followed by sintering the electrode at 723 K for 1 h. The nanostructured TiO_2 film was immersed in the suspension of Au NPs for 12−15 h to optimize the surface coverage of Au NPs. The as-prepared Au/TiO_2 film, after it was rinsed with distilled water, was adsorped in 25 mM phosphate buffer solution (PBS, pH 7.2) that contained 0.2 mM cyt. c for ~30 min at 4 °C in a refrigerator. Hereafter, the cyt. c-modified Au/TiO_2 film will be denoted as Au/TiO_2/cyt. c.

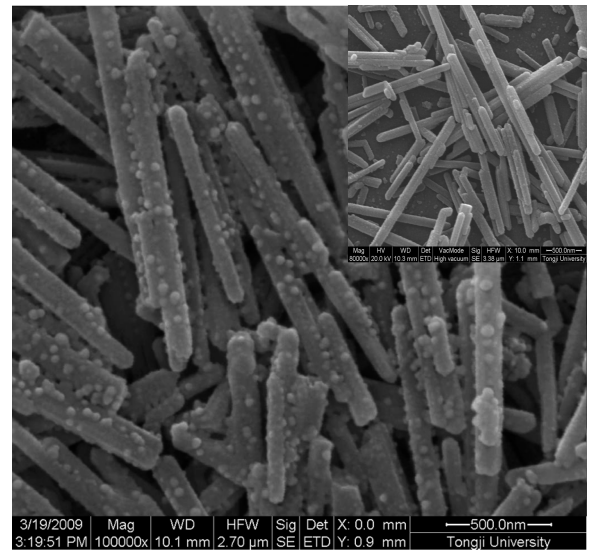

Figure 1. Scanning electron microscopy (SEM) images of the Au/TiO_2 film and the TiO_2 nanoneedle film (inset).

Apparatus and Measurements. The UV−vis absorption spectrum was recorded by an Agilent 8453 UV−vis−NIR spectrophotometer (Agilent Instruments). Scanning electron microscopy (SEM) images of films of TiO_2 needles and Au/TiO_2 nanoneedles were taken by a Quanta 200 FEG (FEI Company). All electrochemical and photoelectrochemical measurements were performed by a computer-controlled CHI 660C electrochemical workstation (Shanghai, PRC) at ambient temperature in a homemade three-electrode cell, using a KCl-saturated Ag|AgCl electrode as the reference electrode and a platinum wire as an auxiliary electrode. The working electrode was irradiated with visible light from the back, using a xenon lamp and a UV cutoff filter (λ > 420 nm). The action spectrum for the photocurrent changes was collected using a xenon lamp with a UV cutoff filter and an appropriate band-pass filter (full width at half maximum (fwhm) = 10 nm). The supporting electrolyte was 25 mM PBS, which was purged with high-purity nitrogen for at least 30 min prior to experiments and a nitrogen atmosphere was maintained over the solution in the cell through the experiments.

RESULTS AND DISCUSSION

Characterization. The morphologies of the TiO_2 nanoneedle film and the Au/TiO_2 film were first characterized using SEM. As demonstrated in Figure 1, the TiO_2 nanoneedles are typically ~50−100 nm in width and ~3−5 μm in length. The Au NPs with diameters of <50 nm are homogeneously dispersed on the surface of TiO_2. The visible absorption spectrum of Au NPs deposited onto the TiO_2 nanoneedle film is clearly characterized by the plasmon resonance peak of Au NPs (540 nm) (see

(12) (a) Tian, Y.; Tatsuma, T. *Chem. Commun.* **2004**, 1810–1811. (b) Tian, Y.; Tatsuma, T. *J. Am. Chem. Soc.* **2005**, *127*, 7632–7637. (c) Yu, K.; Sakai, N.; Tatsuma, T. *Electrochemistry* **2008**, *76*, 161–164.
(13) (a) Takahashi, Y.; Tatsuma, T. *Electrochem. Commun.* **2008**, *10*, 1404–1407. (b) Rodriguez-Gonzales, V.; Zanella, R.; del Angel, G.; Gomez, R. *J. Mol. Catal. A: Chem.* **2008**, *281*, 93–98.
(14) Tian, Y.; Notsu, H.; Tatsuma, T. *Photochem. Photobiol. Sci.* **2005**, *4*, 598–601.
(15) Furube, A.; Du, L.; Hara, K.; Katoh, R.; Tachiya, M. *J. Am. Chem. Soc.* **2007**, *129*, 14852–14853.
(16) Tian, Y.; Wang, X.; Zhang, D.; Shi, X.; Wang, S. *J. Photochem. Photobiol. A* **2008**, *199*, 224–229.
(17) Hedges, D. P.; Richardson, D. J.; Russell, D. A. *Langmuir* **2004**, *20*, 1901–1908.
(18) Brown, K. R.; Walter, D. G.; Natan, M. J. *Chem. Mater.* **2000**, *12*, 306–313.

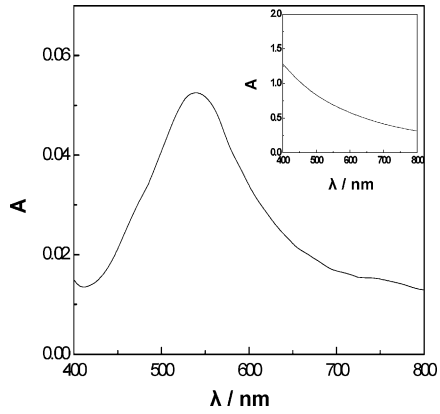

Figure 2. Absorption spectrum corresponding to the Au NPs deposited on the TiO_2 nanoneedle film (the spectrum of TiO_2 needles has been subtracted) and the TiO_2 nanoneedle film (inset).

Figure 2), although it is red-shifted, compared to that of the suspension (530 nm, data not shown), because of the high refractive index of TiO_2.[19] Incidentally, the apparent absorption of the unmodified TiO_2 film in the visible region should be ascribed to light scattering, because the film was not colored before the deposition of gold. Thus, we can conclude that nanosized gold particles were successfully modified onto the TiO_2 nanoneedle film. The position of the Soret absorption band of cyt. c adsorbed on the Au/TiO_2 film was located at 407 nm, just a 2-nm blue shift with that of a native cyt. c solution, which suggests that no obvious denaturation occurred. Moreover, the influence of continuous irradiation with visible light ($\lambda > 420$ nm) on the bioactivity of cyt. c adsorbed on the Au/TiO_2 film was examined up to 3 h and no destructive effect was observed with no shift of the band for cyt. c. These results imply that the Au/TiO_2 film has good biocompatibility and is accessible for cyt. c molecules to maintain their native conformation and bioactivity under plasmon excitation.

Plasmon-Induced Photoelectrochemistry of cyt. c at the Au/TiO_2 Film. Figure 3 shows typical cyclic voltammograms (CVs) of cyt. c at the Au/TiO_2 film without illumination (Figure 3a) and under visible light illumination (Figure 3b) in 25 mM PBS (pH 7.2). As expected, a pair of well-defined redox peaks was observed for both circumstances. The formal potential ($E^{0\prime} = (E_{p,a} + E_{p,c})/2$) of cyt. c at the Au/$TiO_2$ film is estimated to be 39.2 ± 2.4 mV vs Ag|AgCl without illumination and 41.1 ± 2.1 mV with a slight shift under illumination. By integration of the anodic peak in CV, the average surface coverage of electroactive cyt. c adsorbed on the Au/TiO_2 film was estimated to be 5.96×10^{-12} mol cm^2. Cytochrome c might be adsorbed on the Au/TiO_2 film in a monolayer, taking account of the size of the cyt. c molecule.[20] CVs of a Au/TiO_2/cyt. c film with different scan rates were also obtained in the fresh buffer solution, and a linear relationship existed between redox peak currents (I_p^a and I_p^c) and potential scan rate (v), suggesting the surface-confined process (data not shown). Interestingly, both anodic and cathodic redox currents were amplified under visible-light irradiation, whereas no obvious increases in redox currents of cyt. c were observed at the bare TiO_2 nanoneedle film under

(19) Fujishima, A.; Hashimoto, K.; Watanabe, T. *TiO_2 Photocatalysis: Fundamentals and Applications*; BKC: Tokyo, 1999; 125 pp.
(20) Guo, L. H.; Hill, H. A. *Adv. Inorg. Chem.* **1991**, *36*, 341–375.

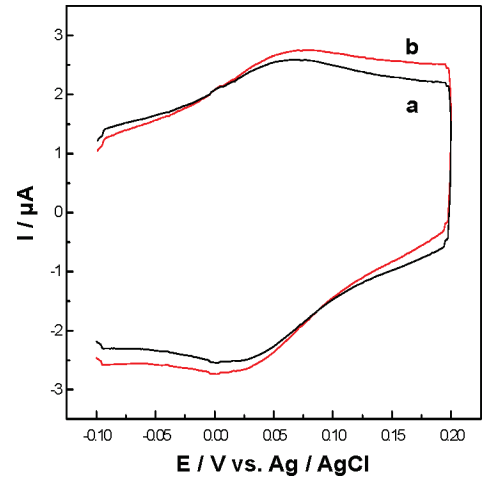

Figure 3. CVs obtained at the Au/TiO_2/cyt. c film (a) without light excitation and (b) under visible-light excitation ($\lambda > 420$ nm, 60 mW/cm^2) in N_2-saturated 25 mM PBS (pH 7.2). Potential scan rate: 100 mV/s.

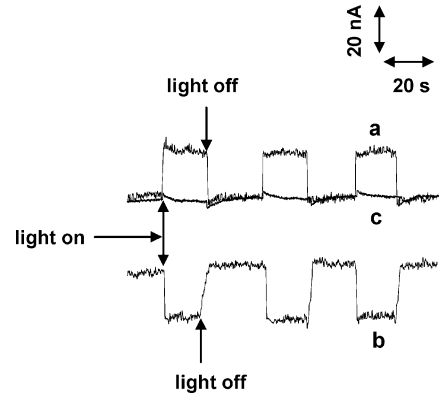

Figure 4. Photocurrents generated by the Au/TiO_2 system in the presence of (a) reduced cyt. c, (b) oxidized cyt. c, and (c) in the absence of cyt. c, at 0 V vs Ag|AgCl upon visible-light illumination ($\lambda > 420$ nm, 60 mW/cm^2) in N_2-saturated 25 mM phosphate buffer solution (pH 7.2).

the same conditions, suggesting the plasmon-induced enhancement in redox currents based on the excitation of gold nanoparticles.

The result was further analyzed by determination of photocurrents by amperometry in the presence of cyt. c at the Au/TiO_2 film upon visible-light irradiation. Figure 4 shows that, in the presence of the reduced cyt. c (Figure 4a), anodic photocurrents are generated under visible light excitation, whereas in the presence of oxidized cyt. c (Figure 4b), cathodic photocurrents are observed at the applied potential of 0 V vs Ag|AgCl, which is close to the formal potential of cyt. c obtained at the Au/TiO_2 film. However, no obvious photocurrents were obtained upon irradiation of the Au/TiO_2 system in the absence of cyt. c (Figure 4c). Herein, cyt. c molecules with a redox active center ($Fe^{2+/3+}$) could provide electrons to the Au/TiO_2 surface under plasmon excitation, resulting in the enhanced photocurrents. Moreover, the redox state of cyt. c controls the direction of photocurrents at the Au/TiO_2 film, and redox currents of cyt. c were amplified by Au NPs under visible-light illumination, as shown in Scheme 1. That is, the cathodic photocurrents are generated by the photoexcited electron

Scheme 1. Photoelectrochemical System Composed of Au/TiO_2 Film and cyt. c: (A) Anodic Photocurrent Generation in the Presence of Reduced cyt. c and (B) Cathodic Photocurrent Generation in the Presence of Oxidized cyt. c

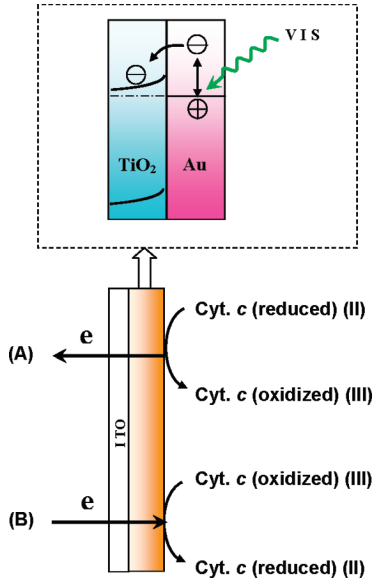

transfer from the Au NPs ascribed to plasmon resonance to the TiO_2 conduction band and the simultaneous electron transfer from the Au/TiO_2 electrode to the oxidized cyt. c. Similarly, the mechanism for the formation of anodic photocurrents involves the transfer of photoexcited electrons from the Au NPs to the TiO_2 conduction band and the simultaneous transfer of compensative electrons from the reduced cyt. c to the Au NPs. Note that, in the absence of Au NPs or TiO_2 nanoneedles, almost no photocurrents were obtained at 0 V vs Ag|AgCl for the electrode in the presence of cyt. c (data not shown), revealing that the enhanced anodic and cathodic photocurrents originate from improved charge separation efficiency in Au/TiO_2 nanoparticles due to the ejection of photoexcited electrons from the Au NPs.

To verify that the enhanced photocurrents are related to the plasmon resonance absorption of Au NPs, the dependence of the generated photocurrents on the wavelength of visible-light irradiation was examined. Action spectrum of photocurrent changes for the Au/TiO_2 film modified with oxidized cyt. c in N_2-saturated 25 mM PBS at 0 V is shown in Figure 5. Control experiments reveal that no obvious photocurrents were observed at the TiO_2 and TiO_2/cyt. c film, because TiO_2 only absorbs light that has a wavelength shorter than 380 nm. In contrast, negative photocurrents were obtained at the Au/TiO_2 film under visible-light illumination. The photocurrent action spectrum follows the spectral feature of Au NPs deposited onto the TiO_2 film. The maximum photocurrent change was also obtained near the absorption peak wavelength of Au NPs. Thus, it was evident that the amplified redox currents are ascribed to the plasmon absorption of Au NPs.

In addition, the CV of the Au/TiO_2/cyt. c film obtained in the fresh buffer solution under visible-light irradiation was maintained essentially unchanged upon consecutive potential scanning up to 300 cycles at 100 mV/s, indicating that cyt. c was stably immobilized onto the Au/TiO_2 nanocomposite surface, even under visible-light illumination.

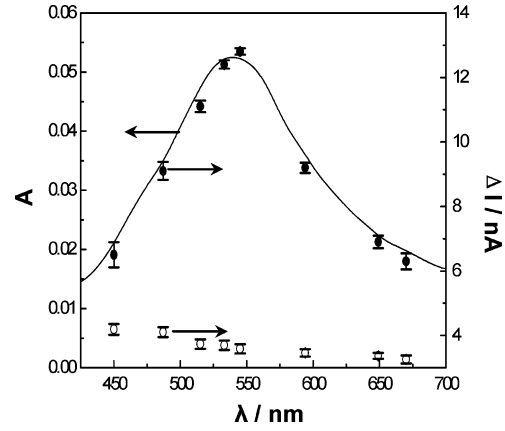

Figure 5. Action spectra of the photocurrent changes generated by (●) the Au/TiO_2/cyt. c film and (○) the TiO_2/cyt. c film, in response to light irradiation (8.52 × 10^{15} photons/cm^2) at 0 V vs Ag|AgCl in N_2-saturated PBS solution. The absorption spectrum of Au NPs on the TiO_2 nanoneedle film is also depicted (solid curves).

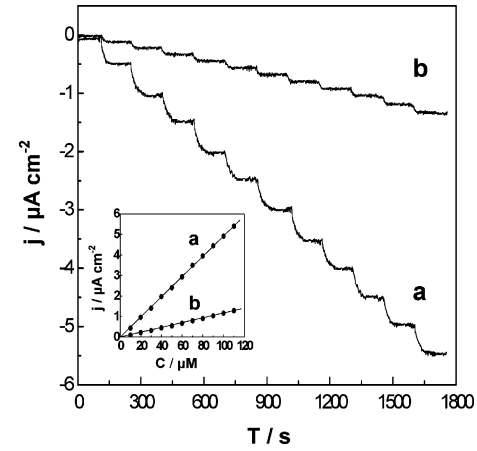

Figure 6. Typical amperometric responses of Au/TiO_2/cyt. c electrode to successive addition of 1 × 10^{-5} M H_2O_2 (a) under visible light illumination (λ > 420 nm, 60 mW/cm^2) and (b) without illumination at 0 V vs Ag|AgCl in 25 mM PBS (pH 7.2). Inset shows the corresponding calibration curves of current density versus the concentration of H_2O_2.

Enhancement in Analytical Performance of the Electrochemical Biosensor. As mentioned previously, both anodic and cathodic redox currents of cyt. c were amplified under visible-light irradiation. Meanwhile, cyt. c was stably immobilized onto the Au/TiO_2 film and processed the enzymatic activity toward H_2O_2, even under visible-light irradiation. Accordingly, a novel photoelectrochemical approach for an assay of H_2O_2 was developed. Amperometric responses of the Au/TiO_2/cyt. c film to successive addition of H_2O_2 (a) under plasmon excitation and (b) without plasmon excitation were conducted at the optimized potential of 0 V vs Ag|AgCl, in which both anodic and cathodic potential interferences could be negligible (data not shown), and the corresponding current−time responses are shown in Figure 6. For control experiments, amperometric response was observed at neither the bare TiO_2 film nor the Au/TiO_2 film under visible-light irradiation upon the addition of H_2O_2. In contrast with other H_2O_2 biosensors reported so far, the present modified electrode under plasmon excitation shows excellent analytical performance, for instance, high sensitivity,

wide dynamic linear range, and low detection limit. Figure 6 clearly shows that the sensitivity of the Au/TiO_2/cyt. c film toward H_2O_2 under plasmon excitation estimated to be 49.4 mA cm^{-2} M^{-1} is 4-fold larger than that generated without excitation. This value is also much greater than that obtained at the cyt. c-modified TiO_2 nanoneedles film reported in our previous work.[21] The dynamic linear detection range was extended to $1 \times 10^{-7}-1.2 \times 10^{-2}$ M, which is wider than that of previous biosensors for H_2O_2, based on direct electron transfer of enzymes on metal oxide surfaces.[21,22] Moreover, the detection limit achieved to be 4.5×10^{-8} M is lower than that of previously reported H_2O_2 biosensors (based on a signal-to-noise ratio of S/N = 3).[23] The Au/TiO_2/cyt. c electrode was stored in a black box at 3 °C in a refrigerator between tests, to avoid UV light irradiation. The response current for H_2O_2 was recorded three times daily, and the current responses had almost no changes for at least half a month, which was indicative of the good stability.

CONCLUSION

A facile and effective plasmon-induced photoelectrochemical strategy for determination of H_2O_2 with enhanced analytical performance has been developed through direct electron transfer of cytochrome c (cyt. c) at a TiO_2 nanoneedle film loaded with gold nanoparticles (Au NPs). Both anodic and cathodic redox currents of cyt. c have been amplified under visible-light irradiation. The enhanced photocurrents are proposed to be generated from the surface plasmon resonance of Au NPs, which has been confirmed by the good match between action spectrum for photocurrent changes and ultraviolet-visible light (UV−vis) adsorption spectrum of Au NPs. In addition, experimental results have demonstrated that cyt. c has been stably immobilized onto the Au/TiO_2 film and maintained its enzymatic activity toward H_2O_2. Accordingly, the photoelectrochemical biosensor for H_2O_2 has been achieved at the Au/TiO_2/cyt. c system with enhanced analytical performance. The sensitivity of the present biosensor is 4-fold larger than that obtained at the Au/TiO_2 film without visible-light illumination. It is first reported that Au NPs can not only provide a favorable microenvironment for immobilized cyt. c to catalyze H_2O_2, but also convert visible-light energy to electric signal, thus enhancing the signal-to-noise ratio. Besides this characteristic, the present biosensor for H_2O_2 has also exhibited a low detection limit, a wide dynamic linear range, and good stability. The present investigation provides an excellent model for determination of biomolecules with enhanced analytical performance by amplifying redox currents of enzymes at the Au/TiO_2 film through surface plasmon resonance. This strategy should also be extended to other metal nanoparticles, such as platinum, copper, and so on.

(21) Luo, Y.; Liu, H.; Rui, Q.; Tian, Y. *Anal. Chem.* **2009**, *81*, 3035–3041.

(22) (a) Zhang, Y.; He, P.; Hu, N. *Electrochim. Acta* **2004**, *49*, 1981–1988. (b) Zheng, W.; Zheng, Y. F.; Jin, K. W.; Wang, N. *Talanta* **2008**, *74*, 1414–1419. (c) Liu, A.; Wei, M.; Honma, I.; Zhou, H. *Anal. Chem.* **2005**, *77*, 8068–8077. (d) Xiao, P.; Garcia, B. B.; Guo, Q.; Liu, D.; Cao, G. *Electrochem. Commun.* **2007**, *9*, 2441–2447. (e) Lu, H.; Yang, J.; Rusling, J. F.; Hu, N. *Electroanalysis* **2006**, *18*, 379–390.

(23) (a) Wang, Y.; Chen, X.; Zhu, J. *Electrochem. Commun.* **2009**, *11*, 323–326. (b) Li, F.; Chen, W.; Tang, C.; Zhang, S. *Talanta* **2009**, *77*, 1304–1308. (c) Chen, S.; Yuan, R.; Chai, Y.; Yin, B.; Li, W.; Min, L. *Electrochim. Acta* **2009**, *54*, 3039–3046. (d) Yang, X.; Chen, X.; Zhang, X.; Yang, W.; Evans, D. G. *Sens. Actuators, B* **2008**, *134*, 182–188. (e) Kafi, A. K. M.; Wu, G.; Chen, A. *Biosens. Bioelectron.* **2008**, *24*, 566–571. (f) Zhang, L.; Zhang, Q.; Li, J. *Adv. Funct. Mater.* **2007**, *17*, 1958–1965. (g) Qiu, J.; Peng, H.; Liang, R.; Li, J.; Xia, X. *Langmuir* **2007**, *23*, 2133–2137. (h) Zhao, G.; Xu, J.; Chen, H. *Anal. Biochem.* **2006**, *350*, 145–150.

ACKNOWLEDGMENT

This work was financially supported by the Program for New Century Excellent Talents in University (NCET-06-0380) and the Scientific Research Foundation for the Returned Overseas Chinese Scholars, from State Education Ministry, China, and Nanometer Science Foundation of Shanghai (0952 nm04900). Tongji University is also greatly acknowledged.

Received for review April 26, 2009. Accepted July 22, 2009.

AC900894P